

Atomistic description of the electronic structure of $\text{In}_x\text{Ga}_{1-x}\text{As}$ alloys and InAs/GaAs superlattices

Kwiseon Kim, P. R. C. Kent, and Alex Zunger
National Renewable Energy Laboratory, Golden, Colorado 80401

C. B. Geller
Bettis Atomic Power Laboratory, West Mifflin, Pennsylvania 15122

Received 12 March 2002; published 30 July 2002)

We show how an empirical pseudopotential approach, fitted to bulk and interfacial reference systems, provides a unified description of the electronic structure of random alloys (bulk and epitaxial), superlattices, and related complex systems. We predict the composition and superlattice-period dependence of the band offsets and interband transitions of InAs/GaAs systems on InP and GaAs substrates.

DOI: 10.1103/PhysRevB.66.045208

PACS number s): 71.20.Nr, 71.15.-m

I. INTRODUCTION

InAs and GaAs are the building blocks of a diverse range of optoelectronic heterojunction systems, including i) short-period superlattices $(\text{InAs})_n$

The various InAs/GaAs systems discussed above (as well as other isovalent and isostructural semiconductor pairs) all

LDA calculations^{54,55} predict a *large negative* $a_c < 0$ deformation potential for the CBM, and small deformation poten-

varied, plane waves are added or subtracted, potentially significantly increasing or decreasing the flexibility of the basis set. In order to minimize this effect, we find it beneficial to apply a weighting function to the individual plane waves

$$w_G = \frac{\cos(\theta) + 1}{2}, \quad (14)$$

$$= \frac{E_G - E_{cut}}{1 - E_{cut}}, \quad (15)$$

where E_G is the kinetic energy of the plane wave $|G + k|^2/2$. We find $\theta = 0.8$ provides an improved fit to cell-shape dependent properties such as hydrostatic and biaxial deformation potentials and alloy properties of strongly

A. Equilibrium atomic positions in superlattices

1. Continuum elasticity (CE) theory for strained superlattices

A film of a material grown epitaxially on a thick substrate will strain so that its atoms grow in registry with those of the substrate. Thus, its dimension a_{\parallel} , the lattice parameter of the layer parallel to the interface, becomes equal to that of the substrate a_s (coherency condition), and a_{\perp} , the lattice parameter of the layer perpendicular to the interface, is determined by the strain tensor. Based on macroscopic continuum elasticity theory,⁶⁷⁻⁶⁹

$$a_{\perp} = a_s (1 - q(\hat{G}) \frac{a_s - a_{eq}}{a_s}), \quad (17)$$

Here, \hat{G} is the direction of deformation and the epitaxial strain reduction factor is given by

$$q(\hat{G}) = 1 - \frac{B}{C_{11} + \Delta(\hat{G})}, \quad (18)$$

where B is the bulk modulus, the C_{ij} are elastic constants of the embedded material, and

$$\Delta = C_{44} - \frac{1}{2} (C_{11} - C_{12}) \quad (19)$$

is the elastic anisotropy. Δ is a purely geometric factor given by

$$\Delta(\hat{G}) = C_{44} (1 + \sin^2 \theta) + \frac{1}{2} (C_{11} - C_{12}) \sin^4 \theta, \quad (20)$$

where θ are the spherical angles formed by \hat{G} . A general expression for $q(\hat{G})$ is given in Ref. 67. Explicit expressions for $q(\hat{G})$ along the principal directions (001), (011), (111), (110), (100), (101), (110), (111), (112), (113), (114), (115), (116), (117), (118), (119), (120), (121), (122), (123), (124), (125), (126), (127), (128), (129), (130), (131), (132), (133), (134), (135), (136), (137), (138), (139), (140), (141), (142), (143), (144), (145), (146), (147), (148), (149), (150), (151), (152), (153), (154), (155), (156), (157), (158), (159), (160), (161), (162), (163), (164), (165), (166), (167), (168), (169), (170), (171), (172), (173), (174), (175), (176), (177), (178), (179), (180), (181), (182), (183), (184), (185), (186), (187), (188), (189), (190), (191), (192), (193), (194), (195), (196), (197), (198), (199), (200), (201), (202), (203), (204), (205), (206), (207), (208), (209), (210), (211), (212), (213), (214), (215), (216), (217), (218), (219), (220), (221), (222), (223), (224), (225), (226), (227), (228), (229), (230), (231), (232), (233), (234), (235), (236), (237), (238), (239), (240), (241), (242), (243), (244), (245), (246), (247), (248), (249), (250), (251), (252), (253), (254), (255), (256), (257), (258), (259), (260), (261), (262), (263), (264), (265), (266), (267), (268), (269), (270), (271), (272), (273), (274), (275), (276), (277), (278), (279), (280), (281), (282), (283), (284), (285), (286), (287), (288), (289), (290), (291), (292), (293), (294), (295), (296), (297), (298), (299), (300), (301), (302), (303), (304), (305), (306), (307), (308), (309), (310), (311), (312), (313), (314), (315), (316), (317), (318), (319), (320), (321), (322), (323), (324), (325), (326), (327), (328), (329), (330), (331), (332), (333), (334), (335), (336), (337), (338), (339), (340), (341), (342), (343), (344), (345), (346), (347), (348), (349), (350), (351), (352), (353), (354), (355), (356), (357), (358), (359), (360), (361), (362), (363), (364), (365), (366), (367), (368), (369), (370), (371), (372), (373), (374), (375), (376), (377), (378), (379), (380), (381), (382), (383), (384), (385), (386), (387), (388), (389), (390), (391), (392), (393), (394), (395), (396), (397), (398), (399), (400), (401), (402), (403), (404), (405), (406), (407), (408), (409), (410), (411), (412), (413), (414), (415), (416), (417), (418), (419), (420), (421), (422), (423), (424), (425), (426), (427), (428), (429), (430), (431), (432), (433), (434), (435), (436), (437), (438), (439), (440), (441), (442), (443), (444), (445), (446), (447), (448), (449), (450), (451), (452), (453), (454), (455), (456), (457), (458), (459), (460), (461), (462), (463), (464), (465), (466), (467), (468), (469), (470), (471), (472), (473), (474), (475), (476), (477), (478), (479), (480), (481), (482), (483), (484), (485), (486), (487), (488), (489), (490), (491), (492), (493), (494), (495), (496), (497), (498), (499), (500), (501), (502), (503), (504), (505), (506), (507), (508), (509), (510), (511), (512), (513), (514), (515), (516), (517), (518), (519), (520), (521), (522), (523), (524), (525), (526), (527), (528), (529), (530), (531), (532), (533), (534), (535), (536), (537), (538), (539), (540), (541), (542), (543), (544), (545), (546), (547), (548), (549), (550), (551), (552), (553), (554), (555), (556), (557), (558), (559), (560), (561), (562), (563), (564), (565), (566), (567), (568), (569), (570), (571), (572), (573), (574), (575), (576), (577), (578), (579), (580), (581), (582), (583), (584), (585), (586), (587), (588), (589), (590), (591), (592), (593), (594), (595), (596), (597), (598), (599), (600), (601), (602), (603), (604), (605), (606), (607), (608), (609), (610), (611), (612), (613), (614), (615), (616), (617), (618), (619), (620), (621), (622), (623), (624), (625), (626), (627), (628), (629), (630), (631), (632), (633), (634), (635), (636), (637), (638), (639), (640), (641), (642), (643), (644), (645), (646), (647), (648), (649), (650), (651), (652), (653), (654), (655), (656), (657), (658), (659), (660), (661), (662), (663), (664), (665), (666), (667), (668), (669), (670), (671), (672), (673), (674), (675), (676), (677), (678), (679), (680), (681), (682), (683), (684), (685), (686), (687), (688), (689), (690), (691), (692), (693), (694), (695), (696), (697), (698), (699), (700), (701), (702), (703), (704), (705), (706), (707), (708), (709), (710), (711), (712), (713), (714), (715), (716), (717), (718), (719), (720), (721), (722), (723), (724), (725), (726), (727), (728), (729), (730), (731), (732), (733), (734), (735), (736), (737), (738), (739), (740), (741), (742), (743), (744), (745), (746), (747), (748), (749), (750), (751), (752), (753), (754), (755), (756), (757), (758), (759), (760), (761), (762), (763), (764), (765), (766), (767), (768), (769), (770), (771), (772), (773), (774), (775), (776), (777), (778), (779), (780), (781), (782), (783), (784), (785), (786), (787), (788), (789), (790), (791), (792), (793), (794), (795), (796), (797), (798), (799), (800), (801), (802), (803), (804), (805), (806), (807), (808), (809), (810), (811), (812), (813), (814), (815), (816), (817), (818), (819), (820), (821), (822), (823), (824), (825), (826), (827), (828), (829), (830), (831), (832), (833), (834), (835), (836), (837), (838), (839), (840), (841), (842), (843), (844), (845), (846), (847), (848), (849), (850), (851), (852), (853), (854), (855), (856), (857), (858), (859), (860), (861), (862), (863), (864), (865), (866), (867), (868), (869), (870), (871), (872), (873), (874), (875), (876), (877), (878), (879), (880), (881), (882), (883), (884), (885), (886), (887), (888), (889), (890), (891), (892), (893), (894), (895), (896), (897), (898), (899), (900), (901), (902), (903), (904), (905), (906), (907), (908), (909), (910), (911), (912), (913), (914), (915), (916), (917), (918), (919), (920), (921), (922), (923), (924), (925), (926), (927), (928), (929), (930), (931), (932), (933), (934), (935), (936), (937), (938), (939), (940), (941), (942), (943), (944), (945), (946), (947), (948), (949), (950), (951), (952), (953), (954), (955), (956), (957), (958), (959), (960), (961), (962), (963), (964), (965), (966), (967), (968), (969), (970), (971), (972), (973), (974), (975), (976), (977), (978), (979), (980), (981), (982), (983), (984), (985), (986), (987), (988), (989), (990), (991), (992), (993), (994), (995), (996), (997), (998), (999), (1000)

$$C_{11} + 2C_{12} = \sqrt{\quad}$$

$\rightarrow\infty$ are shown as dashed lines in Fig. 2. We see that continuum elasticity also works well for the c/a ratio.

4. VFF vs LDA for superlattices

As a simple test of our GVFF for alloy systems, we compared the relaxed atomic positions from GVFF with pseudopotential LDA results for a (100) $(\text{GaAs})_1/(\text{InAs})_1$ superlattice where the c/a ratio is fixed to 1, but we allow energy minimizing changes in the overall lattice constant (a_{eq}) and the atomic internal degrees of freedom (u_{eq}). We find

$$a_{eq}^{LDA} = 5.8612 \text{ \AA},$$

$$u_{eq}^{LDA} = 0.2305,$$

while the GVFF results are

$$a_{eq}^{GVFF} = 5.8611 \text{ \AA},$$

$$u_{eq}^{GVFF} = 0.2305.$$

A first-principles calculation by Bernard and Zunger⁶⁵ for $(\text{InAs})_1(\text{GaAs})_7$ (001) superlattice resulted in $\epsilon_{\perp} = 7.73\%$. Our GVFF gives 7.36%.

5. Atomic relaxation and interlayer spacing in InAs/GaAs superlattices

Figure 3 shows (001) and (111) interlayer distances in $(\text{GaAs})_8/(\text{InAs})_8$ superlattices. For an unrelaxed (001) superlattice, the internal coordinate z of the indium plane is 0.25 with respect to the c axis. The strain $\epsilon_{\perp} = (z - z_{equil})/z_{equil}$ is shown in Fig. 3. For an

We see that on a GaAs substrate, the atoms of the GaAs segment of the superlattice (SL) are unrelaxed, whereas the strain in the InAs segment is positive. Most atoms have constant strain, except the atoms next to the interface. On the other hand, on an InP substrate, the GaAs segment is dilated ($\epsilon_{\perp} < 0$) and the InAs segment is compressed ($\epsilon_{\perp} > 0$), even though the lattice constant of the SL is almost matched to that of the substrate.

B. Equilibrium atomic positions in random alloys

The GVFF also is used to determine equilibrium atomic positions in random alloys. Here we create a supercell and randomly occupy cation sites with Ga and In atoms, according to the concentration $\text{In}_{1-x}\text{Ga}_x\text{As}$. We then minimize the GVFF elastic energy by displacing atoms to their relaxed positions. We use a conjugate gradient algorithm using analytically calculated forces for both atomic positions and a_{\perp} . In a previous study⁶⁶ we reported the results for the closely related $\text{In}_{1-x}\text{Ga}_x\text{P}$ alloy, so we will not repeat the results for $\text{In}_{1-x}\text{Ga}_x\text{As}$ here. In both cases we find a bimodal distribution of the nearest-neighbor anion-cation bond lengths, and a multimodal distribution of the cation-cation distances. Details are given in Ref. 66.

IV. STRAIN-MODIFIED BAND OFFSETS

Once we have determined the equilibrium atomic positions, and have a reliable screened pseudopotential, we can solve the Schrödinger equation, Eq. 3), in the plane-wave basis of Eq. 5). We first solve the simplest case, epitaxially deformed InAs and GaAs. Here, we imagine that GaAs is coherently strained on a substrate whose lattice constant a_s ranges from that of GaAs to that of InAs. The tetragonal deformation $a_{\perp}(a$

InAs/GaAs band offsets for various substrates such as GaAs, InP, and InAs. The calculated strained offsets on these substrates are given in Fig. 5 for two orientations, (001) and (111).

V. BAND-EDGE STATES IN RANDOM $\text{In}_x\text{Ga}_{1-x}\text{As}$ ALLOYS

Figure 6 shows the band-edge states and the band gaps of a) relaxed “bulk”) $\text{In}_x\text{Ga}_{1-x}$

crossover¹⁵ around 50% In, and a very shallow offset, sug-

CBM / VBM levels and bandgap energies for $(\text{GaAs})_n(\text{InAs})_n$ SL

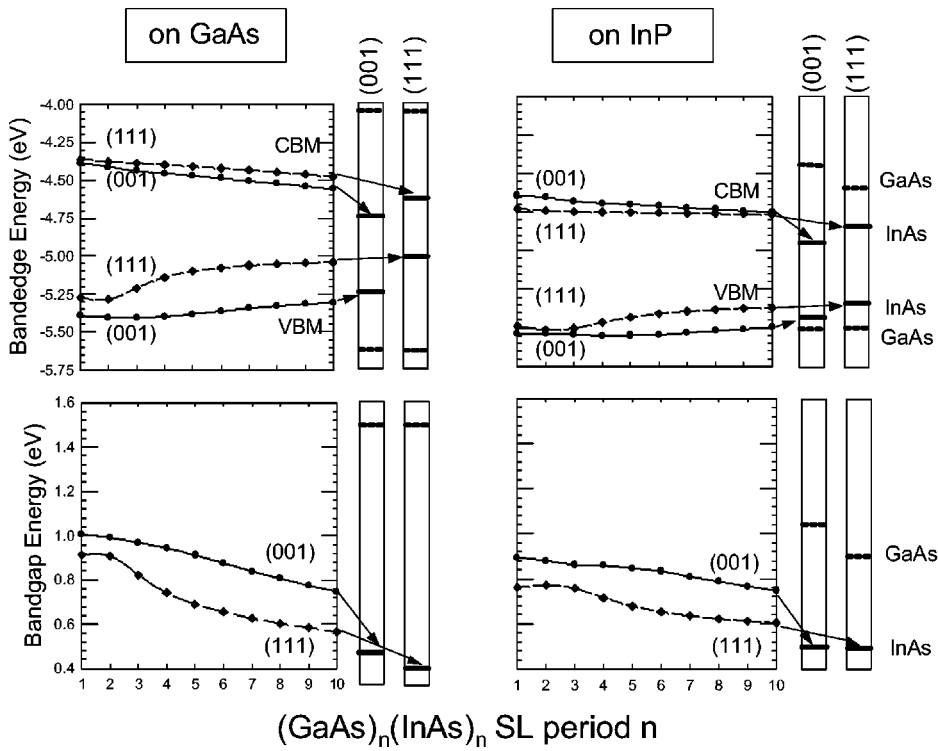


FIG. 7. The CBM and VBM levels for 001) and 111) $(\text{GaAs})_n(\text{InAs})_n$ superlattices on GaAs and InP. The boxes on the right-hand side of each panel depict the band edges of pure GaAs (dashed lines) and pure InAs (solid lines) binaries strained epitaxially on the corresponding substrate for the corresponding orientation. The two lower panels depict the band gaps.

CBM / VBM levels and bandgap energies for $(\text{GaAs})_n(\text{InAs})_1$ SL

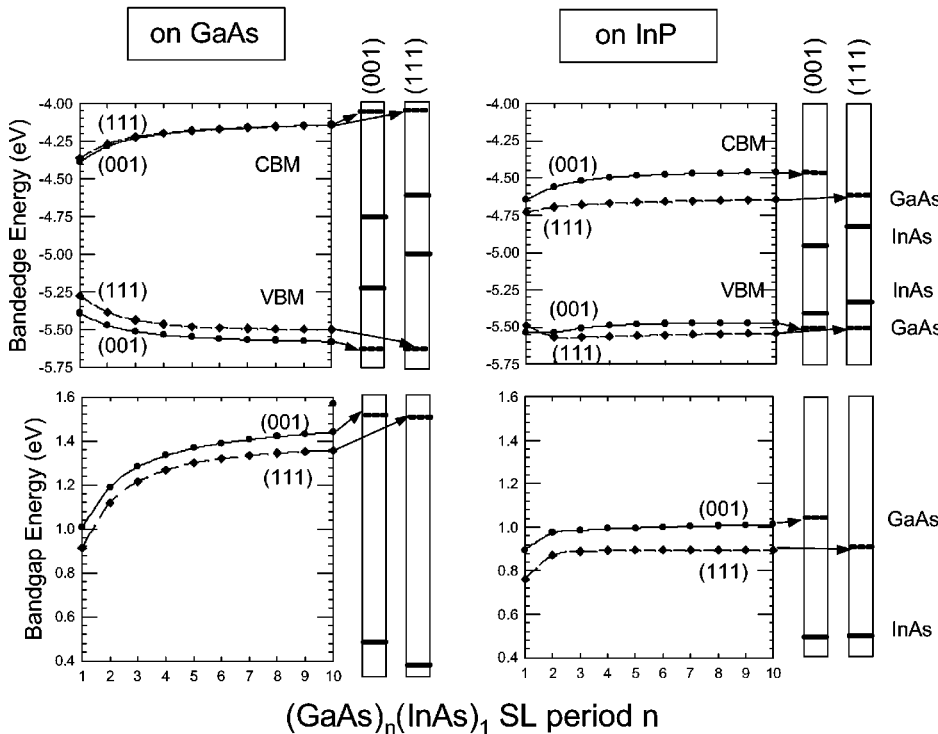


FIG. 8. The CBM and VBM levels and band gaps for 001) and 111) $(\text{GaAs})_n(\text{InAs})_1$ superlattices on GaAs and InP. The boxes on the right-hand side of each panel depict the band edges of pure GaAs and pure InAs binaries strained epitaxially on the corresponding substrate for the corresponding orientation.

of the (001) $(\text{GaAs})_n(\text{InAs})_n$ superlattice on InP for $n = 2, 6,$ and 10 . For the largest period shown, $n = 10$, the CBM states are localized on InAs, just as in the asymptotic behavior noted in Fig. 6. However, for shorter periods, Fig. 10 shows

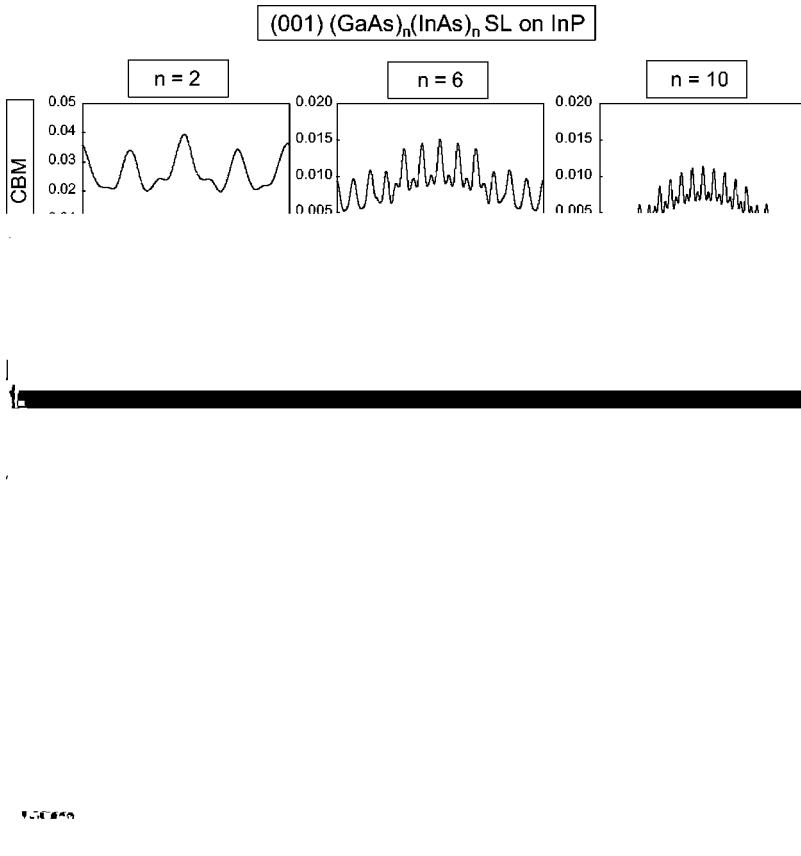


FIG. 10. The planar average of wave functions for (001) $(\text{GaAs})_n(\text{InAs})_n$ SL on InP for periods $n=2,6,10$ and for the states CBM, lh1, hh1, and hh2.

APPENDIX A: CALCULATION OF THE LOCAL STRAIN

To use the empirical pseudopotential, one needs a method to calculate the local strain for arbitrary systems. Figure 12 illustrates how the local strain is calculated. After the atomic positions are relaxed by minimizing the elastic energy, the

local strain tensor ϵ_{ij} is calculated at each atomic site by considering the tetrahedron formed by the four nearest neighbor atoms. The distorted tetrahedron edges, $\mathbf{R}_{12}, \mathbf{R}_{23}$, and \mathbf{R}_{34} are related to the ideal tetrahedron edges $\mathbf{R}_{12}^0, \mathbf{R}_{23}^0$, and \mathbf{R}_{34}^0 via which

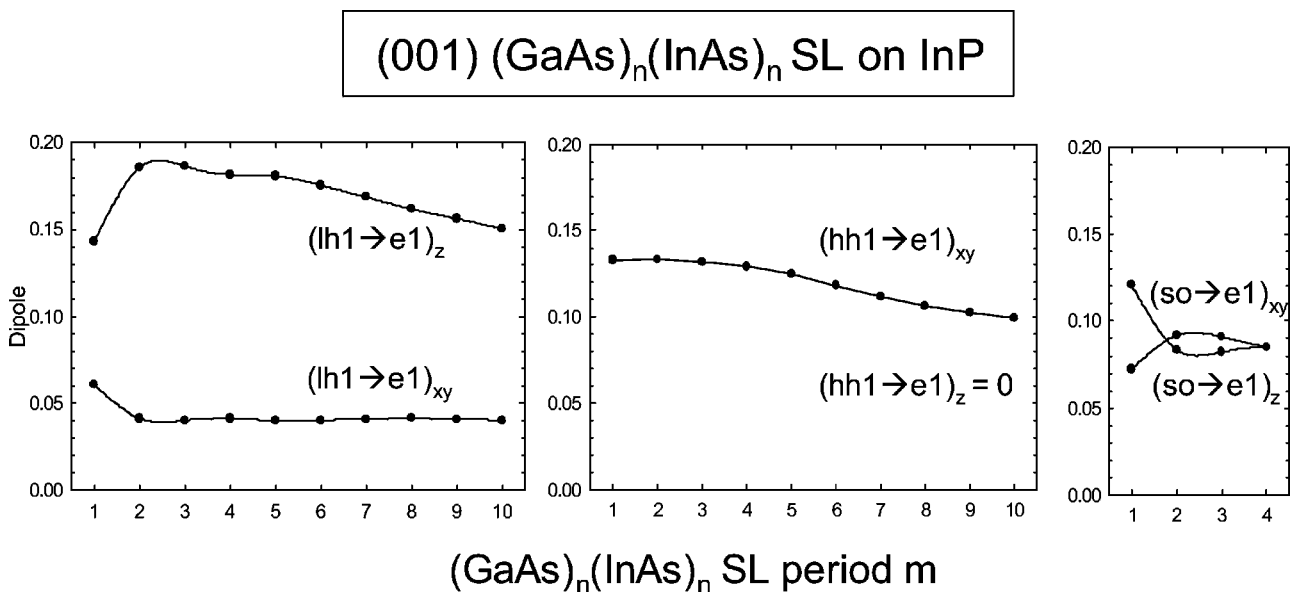


FIG. 11. The dipole elements for interband transitions in (001) $(\text{GaAs})_n(\text{InAs})_n$ SL on InP.

$$\begin{pmatrix} R_{12,x} & R_{23,x} & R_{34,x} \\ R_{12,y} & R_{23,y} & R_{34,y} \\ R_{12,z} & R_{23,z} & R_{34,z} \end{pmatrix} = \begin{pmatrix} 1 + \epsilon_{xx} & \epsilon_{yx} & \epsilon_{zx} \\ 1 + \epsilon_{xy} & 1 + \epsilon_{yy} & \epsilon_{zy} \\ \epsilon_{xz} & \epsilon_{yz} & 1 + \epsilon_{zz} \end{pmatrix} \\
\times \begin{pmatrix} R_{12,x}^0 & R_{23,x}^0 & R_{34,x}^0 \\ R_{12,y}^0 & R_{23,y}^0 & R_{34,y}^0 \\ R_{12,z}^0 & R_{23,z}^0 & R_{34,z}^0 \end{pmatrix}. \quad \text{A1)}$$

The ideal tetrahedron edges are $\{\mathbf{R}^0\} = \{[110]a/2, [0\bar{1}1]a/2, [\bar{1}10]a/2\}$, where a denotes the equilibrium lattice constant. The local strain, ϵ_{ij} is then calculated by a matrix inversion as

- Superlattices Microstruct. **3**, 539 (1987).
- ¹⁹S.H. Pan, H. Shen, Z. Hany, F.H. Pollak, W. Zhuang, Q. Xu, A.P. Roth, R.A. Masut, C. Lancelle, and D. Morris, Phys. Rev. B **38**, 3375 (1988).
- ²⁰J.Y. Marzin and E.V.K. Rao, Appl. Phys. Lett. **43**, 560 (1983).
- ²¹A. Zunger, MRS Bull. **23**, 35 (1998).
- ²²M. Grundmann, D. Biernberg, and N. N. Ledentson, *Quantum Dot Heterostructures* Wiley, New York, 1998).
- ²³T. Lundstrom, W.V. Schoenfeld, H. Lee, and P.M. Petroff, Science **286**, 2312 (1999).
- ²⁴R.G. Dandrea and A. Zunger, Phys. Rev. B **43**, 8962 (1991).
- ²⁵D.L. Smith and C. Mailhot, Rev. Mod. Phys. **62**, 173 (1990).
- ²⁶Y.C. Chang and J.N. Schulman, Appl. Phys. Lett. **43**, 536 (1983).
- ²⁷L.J. Sham and Y.T. Lu, J. Lumin. **44**, 207 (1989).
- ²⁸G. Edwards and J.C. Inkson, Solid State Commun. **89**, 595 (1994).
- ²⁹K.A. Mader and A. Zunger, Phys. Rev. B **50**, 17 393 (1995).
- ³⁰D.M. Wood and A. Zunger, Phys. Rev. B **53**, 7949 (1996).
- ³¹L.W. Wang, S.H. Wei, T. Mattila, A. Zunger, I. Vurgaftman, and J.R. Meyer, Phys. Rev. B **60**, 5590 (1999).
- ³²R. Magri, L.W. Wang, A. Zunger, I. Vurgaftman, and J.R. Meyer, Phys. Rev. B **61**, 10 235 (2000).
- ³³D. Gershoni, C.H. Henry, and G.A. Baraff, IEEE J. Quantum Electron. **29**, 2433 (1993).
- ³⁴M.G. Burt, J. Phys. C **4**, 6651 (1992).
- ³⁵L.R. Ram-Mohan, K.H. Yoo, and R.L. Aggarwal, Phys. Rev. B **38**, 6151 (1988).
- ³⁶A. B. Chen and A. Sher, *Semiconductor Alloys* Plenum, New York, 1995).
- ³⁷A. Zunger, S.-H. Wei, L.G. Ferreira, and J. Bernard, Phys. Rev. Lett. **65**, 353 (1990).
- ³⁸J.E. Bernard and A. Zunger, Phys. Rev. B **36**, 3199 (1987).
- ³⁹R. Magri, S. Froyen, and A. Zunger, Phys. Rev. B **44**, 7947 (1991).
- ⁴⁰S.-H. Wei and A. Zunger, Phys. Rev. B **43**, 1662 (1991).
- ⁴¹S.-H. Wei and A. Zunger, Phys. Rev. Lett. **76**, 664 (1996).
- ⁴²P.R.C. Kent and A. Zunger, Phys. Rev. Lett. **86**, 2613 (2001).
- ⁴³*Electronic Density Functional Theory*, edited by J. F. Dobson, G. Vignale, and M. P. Das Plenum, New York, 1996).
- ⁴⁴L. Hedin, J. Phys. C **11**, 489 (1999).
- ⁴⁵P. Hohenberg and W. Kohn, Phys. Rev. **136**